

Synthesis of nanocrystalline NASICON-type thin film ceramics

Paul A. Lessing* and Gary Huestis

Idaho National Laboratory P.O. Box 1625 Idaho Falls, Idaho 83415-2218, USA

Experiments were conducted to fabricate nano-crystalline ceramic thin films (membranes) using polymeric resin precursors. Two different NASICON compositions were chosen for fabrication: (1) $\text{NaZr}_2\text{Si}_x\text{P}_{3-x}\text{O}_{12}$, and (2) $\text{Na}_{1+x}\text{Sn}_{2-x}\text{In}_x\text{P}_3\text{O}_{12}$. Zirconium-containing resins could not be synthesized without precipitations; however, clear resins were successfully generated using a tin-based composition ($\text{NaSn}_2\text{P}_3\text{O}_{12}$). The tin-based resins were spin-coated onto silicon substrates and then heated (calcined) to high temperatures using ozone as an oxidant. Optimum resin viscosity, spin coating, and calcination conditions were developed. The resulting thin films were characterized using X-ray diffraction (XRD) and Transmission Electron Microscopy (TEM) techniques. Fully-oxidized, single phase, crack-free films were generated that were approximately 80-100 nanometres thick containing crystalline grains about 5-10 nanometres in diameter after calcining at temperatures of about 600 °C to 700 °C. These grain sizes did not correlate with those measured in "chunks" of resins that were calcined using the same conditions. Therefore, thin films of the Sn-NASICON precursor coatings appear to provide physical constraints that are conducive to the formation of nano-crystals at temperatures of about 600 °C to 700 °C. Enhanced transport of the ions in the nano-crystalline grain boundaries at relatively low temperatures is predicted. The films should prove suitable for ion exchange of the sodium ions with protons where the resulting enhanced conductivity could lead to practical devices, including: hydrogen separation membranes, fuel cells, hydrogen "pumps", electrolyzers, thermoelectric generators, electrochemical reactors, and sensors.

Key words: inorganic membrane, nano-crystalline, thin-film, NASICON, proton.

Introduction

Fast ion-conducting materials have been the subject of extensive research because of their potential use in electrochemical devices such as batteries, fuel cells, thermoelectric generators (e.g. Alkali Metal Thermal Electric Converter = AMTEC), electrochemical reactors, chemical sensors, and electrochemical displays. Ions of interest include O^{2-} , Li^+ , Na^+ , and H^+ (protons; usually as part of hydronium or hydroxide ions). In order to reduce electrical resistance, there is additional impetus to fabricate these materials as thin film membranes. Our interest is in the fabrication of inorganic ceramic films that are thin, dense, contain extremely fine polycrystalline grains (nano-crystalline), and primarily are ionic conductors (low electronic conductivity).

Nano-crystalline ceramic films contain an exceptional number of grain boundaries, and therefore it is expected that grain boundaries will dominate the material's behavior. One practical example of this behavior is diffusion in nano-crystalline ceramics that occurs much faster along grain boundaries than through the lattice. This is because diffusion is often enhanced within the disordered domain interfaces (grain boundaries). In equiaxed nano-crystals

(5-10 nm diameter), the disordered region between crystallites is comparable to the volume of the crystallite region. Recent reports demonstrate greatly enhanced oxygen ion conduction in ceramic membranes (for use in solid oxide fuel cell applications) with very fine grains [1, 2]. At moderate temperatures, grain boundary diffusion can be more than 1,000 times faster than lattice diffusion.

A fabrication challenge is to restrain grain growth during high temperature densification processes (e.g. sintering) such that the crystallites remain nano-size after the processing. Another challenge is maintaining chemical and physical stability. Some proton-conducting glasses achieve high proton mobility due to incorporation of water (bonded to POH groups). These glasses can be fabricated by sol-gel techniques at low temperatures. However, the gels are deliquescent and also are easily fractured into pieces when heated [3]. This limits the practical application of these glasses to low temperatures and therefore limits the flux values of hydrogen that can be achieved. Fabrication of proton-exchanged β -alumina compositions is difficult because waters of hydration are lost during firing and therefore the crystal structure is irreversibly destroyed [4]. One approach used to solve this problem, for β -alumina, has been to fabricate a potassium ion crystal structure by firing to high temperatures. Then, at room temperature, protons can be electrochemically ion exchanged into the crystals from a mineral acid [5, 6]. Since the potassium

*Corresponding author:
Tel : +1-208-526-8876
Fax: +1-208-526-0690
E-mail: Paul.Lessing@inl.gov

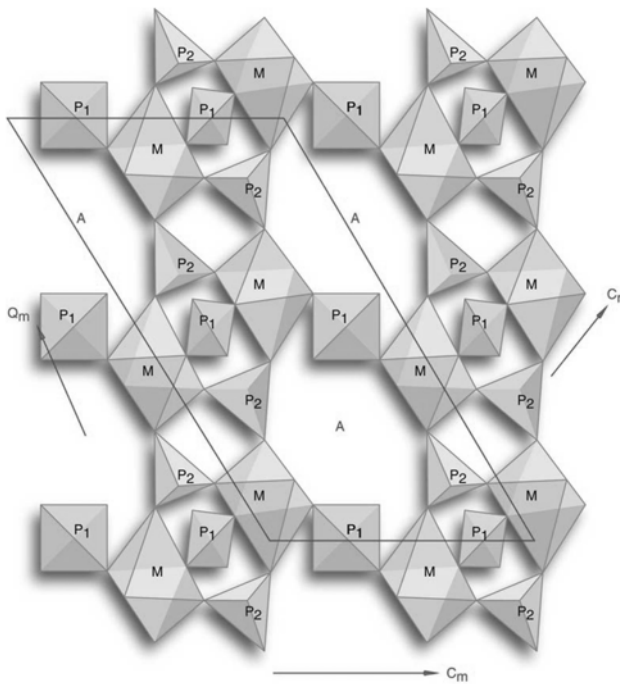


Fig. 1. A generic NASICON Crystal Structure. It is a three-dimensional arrangement of ZrO_6 octahedra (P_1) linked to SiO_4 or PO_4 tetrahedra (P_2) by corner-shared oxygens. The Na^+ or K^+ ions are located in the interstitial sites, "A", formed by the network. The "M" octahedral sites can be occupied by cations such as Zr or Ti, Hf, or Sn.

ion is larger than the sodium ion, using the potassium composition lessens lattice strain during the proton exchange process. In these oxide ceramics, two protonic species can exist. The first type is an H_2O molecule associated with a proton as a hydronium ion (H_3O^+). The second type is a proton bound to an oxygen ion of the crystal lattice ($=OH^+$).

Ion exchange techniques have also been applied to compositions of the family of three-dimensional sodium ion conducting "NASICON". The crystal structure of "NASICON" is shown in Fig. 1.

NASICON is a three dimensional conductor, whereas β -alumina is a two-dimensional conductor. NASICON membranes have primarily been used for efficiently producing caustic (NaOH) from concentrated sodium salts dissolved in water [7]. NASICON is a family of compositions; the original NASICONs were solid solutions derived from $NaZr_2P_3O_{12}$ by partial replacement of P by Si with Na excess to balance the negative charges to generate the formula $Na_{1+x}Zr_2P_{3-x}Si_xO_{12}$ ($0 \leq x \leq 3$). NASICON compositions have been prepared by a sol-gel route, and then the membranes ion exchanged with hydronium ions [8]. However, severe difficulties with cracking of dense membranes occur during the ion-exchange [9]. Recently, a sintered proton-exchanged NASICON-type composition known as PRONASTM has become available in experimental quantities from a commercial supplier [10]. This material was designed for use in liquid systems, but reportedly has been tested

as a membrane for hydrogen gas separation. Presumably, the PRONASTM composition was sintered and then proton-exchanged at room temperature; however, no chemical composition or processing details are available at this date.

Chemical precursor solutions (e.g. sol-gel techniques [11, 12]) have been used to fabricate NASICON structures with well-mixed cations. The resultant materials have often been in a sub-micrometre powder form. The powder can then be densified via sintering or hot-pressing. However, some attempts have been made to utilize sol-gel techniques to form thin films [1]. In addition to sol-gel, polymeric precursors can also be used to generate complex, mixed-cation oxide ceramics. Lessing [2] showed that mixed cation oxide crystallites could be formed from a chelated polymer gel in an expanded structure with a crystallite size of 40-60 nm (after calcining in air at 750 °C). Even smaller grain sizes are anticipated if calcination could be conducted at lower temperatures. However, special steps would be necessary to completely oxidize the carbon resulting from the polymer precursor. Increasing the film thickness can be achieved by increasing the viscosity of the polymeric precursor, spinning at lower speeds, or multiple castings. However, films thicker than about 0.2 micrometre (200 nanometres) have been known to crack, due to shrinkage stresses during calcination.

Experimental

Experiments were conducted to develop synthesis routes for sodium-ion "NASICON" using polymeric-precursors that could be formed into thin films using methods such as spin-casting.

Two different NASICON compositions were chosen for fabrication, using polymer resin precursors: (1) $NaZr_2Si_xP_{3-x}O_{12}$, and (2) $Na_{1+x}Sn_{2-x}In_xP_3O_{12}$.

The first composition represents a traditional composition containing zirconium (Zr). It was anticipated that this type of composition could pose difficulties due to complexities in the Zr chemistry, which can lead to precipitation of unwanted compounds such as zirconium phosphate. Therefore, a second composition was chosen, that would eliminate the zirconium. Partial metal substitution at the octahedral metal site gives the formula $Na_{1+x}Zr_{2-x}M_xP_3O_{12}$, where M could be a wide combination of trivalent metal cations. For indium, there are reports of a solid solution for $Na_{1+x}Zr_{2-x}In_xP_3O_{12}$, with $0 \leq x \leq 1.8$, which could nearly eliminate the Zr from the formula. Or, as reported by Losilla et al. [1], the Zr^{+4} can be replaced by M^{+4} cations such as Sn, Ti, Hf, etc. that can form the necessary octahedral structures. These cations also change the size of the bottlenecks between M1 and M2 (see Fig. 1), and thus can aid the ionic (e.g. sodium, or proton) conductivity. Losilla et al. also reported that increasing indium content (increase x) is concurrent with an increase in Na cation

content, which increases the Na^+ mobility for increased conductivity. Losilla also reported a “thick” grain boundary whose resistance (possibly due to pellets that weren't fully densified) dominated the Z'' spectrum and comprised the major part of the total electrical resistance of his samples at 297 K.

We chose to replace the Zr (ionic radius = 0.72 Å) completely with Sn (ionic radius = 0.69 Å) because Sn has more moderate reactivity properties and would be less prone to premature reactions and precipitations prior to bonding (chelating) with the polymers of the resin precursor. We chose not to include indium in our initial study in order to simplify the chemistry. The resulting films were then heat-treated (calcined in oxidizing atmospheres) to create ceramic films. The ceramic films were characterized with regard to their morphological, microstructural, and crystallinity properties. By controlling the nucleation and growth process at approximately 400-700 °C, while using ozone as the oxidant, it was anticipated that nano-sized crystallites could be achieved in a continuous, dense thin film.

A representation of the process developed at INEEL is shown in Fig. 2.

For the first composition, NASICON synthesis was conducted using the polymeric precursor method for zirconium-containing compositions. Zirconyl nitrate, sodium nitrate, and tri-sodium phosphate were used per

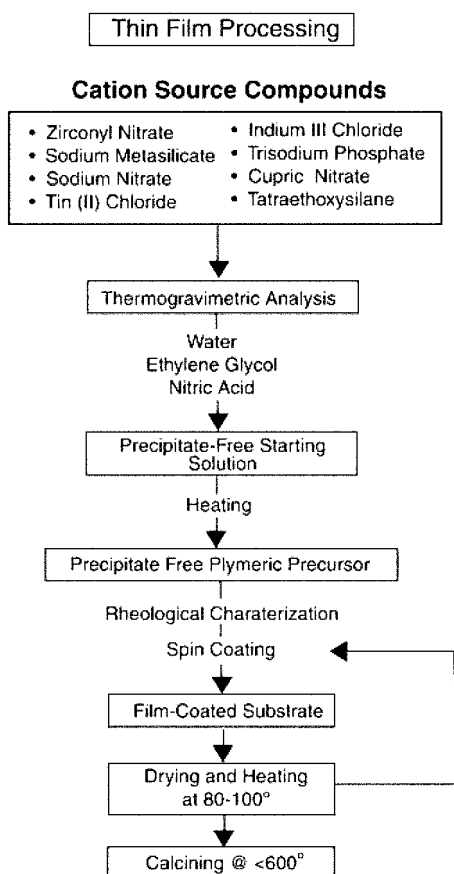


Fig. 2. Flow chart showing the thin film development process.

the method outlined in Fig. 2. The primary concern being the strong affinity of zirconium for phosphate in a solution that could produce a precipitate. However, it was hoped that with enough holding time of separate solutions at 80 °C, the zirconium and the phosphorus would chelate to the citric or oxalic acid so well that when all the solutions were combined, no precipitation or gel formation would occur. After various attempts at varying parameters such as reaction time and concentration of citric acid, use of chloride compounds instead of nitrate compounds, and combining the compounds in different sequences, it was confirmed that some precipitation or gel formation could not be prevented once all of the compounds were combined.

High alkalinity is a major factor in reducing the chance that gel formation will occur. Therefore, sodium hydroxide was used to replace sodium nitrate. Results of this test showed that, after heating the sodium, phosphorus, and zirconium components separately for about three hours and then combining them, precipitation and finally gel formation still occurred. This means that not enough sodium hydroxide was available to maintain a high pH condition such that gel formation would be prevented.

Figure 3 shows the flow chart for the solution preparations for the tin-containing compositions. In sol 1, water was used to dissolve the NaNO_3 (104:1 molar ratio). Ethylene glycol was then added (EG: NaNO_3 = 67:1) as well as citric acid (CA: NaNO_3 = 0.08:1) were combined and heated for 22 hours. In sol 2, ethylene glycol, and citric acid were added to SnCl_2 (34:0.04:1 molar ratio) were combined and heated for the same length of time and temperature as described for sol 1. Four drops of concentrated HNO_3 , using a glass Pasteur pipette, were added to Sol 1 and Sol 2 prior to heating. After the 22-hour heating period, sol 1 and sol 2 were combined and was designated sol 2A.

Sol 2A, which contains both tin and sodium, was heated at 80 °C for 36 hours. Sol 3, which contains H_3PO_4 , ethylene glycol, water and citric acid (E.G.: C.A.: H_3PO_4 = 17:0.03:1) was heated for 24 hrs at 80 °C. Sol 3 was combined with Sol 2A after the 24 hr. heating period. This final combined solution was

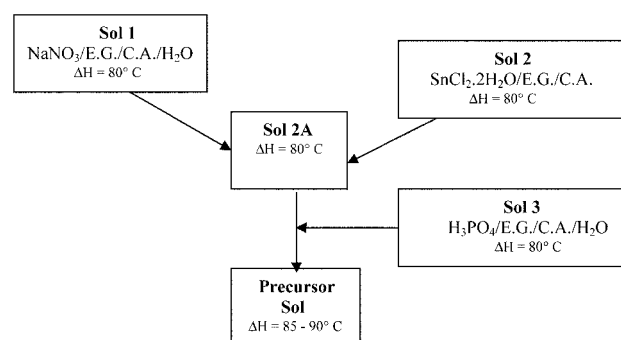


Fig. 3. Flow chart for the synthesis of sodium tin phosphate precursor solution.

designated the Precursor Sol.

The precursor Sol was heated at 85-90 °C for 42 hours. Two thin film preparations were made after that time. The remainder of the solution was then heated at the same temperature for another 17 hours to increase the viscosity for spin coating.

Spin-coated samples were prepared at this point and the remaining liquid precursor resin was calcined to produce powder for x-ray diffraction analysis. Single and multi-layer films were deposited from fresh and aged precursor solutions (up to one week) on silicon and alumina substrates by spin coating. Prior to spinning, the precursor resin solution was measured for a viscosity value with the use of a viscometer (Schott Model ViscoEasy-L). Viscosity measurements are outlined in the results section.

The spin rate and time intervals used in the spin coating apparatus (Chemat KW-4A) were varied to optimize film thickness to be less than 0.5 mm and minimize the effect of film cracking. Spinning speed varied from a minimum rate of 5000 RPM to a maximum rate of 6500 RPM. Spin times were either set for 60 seconds or 120 seconds. Coating quality depended mostly on the cleanliness of the substrate surface. Best coating results came from substrates that were baked out at 400 °C in a tube furnace for four hours with an ozone atmosphere prior to thin film application. This procedure was intended to minimize the effects of carbon contamination on the film surface and probably created a very thin layer of oxidized silicon at the surface. It was further speculated that this oxidized surface would increase the wetting of the precursor solutions.

The substrate surfaces were flooded with precursor resin solution by using a disposable Pasteur pipette. After the prescribed spinning time was completed, the coated substrate was then heat-treated on a hot plate for approximately 10 minutes at 85-90 °C to "set" the thin film. The substrates with films were then placed in an oven at 81 °C over night to slowly bake out the volatile compounds. The next step was a 320 °C heat treatment for four hours in a tube furnace (Lindberg Blue M Model STF5644346) containing an ozone atmosphere. Ozone was used in an attempt to oxidize the carbonaceous material at temperatures low enough to minimize grain growth. The ozone-rich atmosphere was set to a concentration of 112 µg of O₃/mL of O₂ at an oxygen flow rate of 31 millilitres per minute. An OZONELAB 100DS ozone generator was used. The final step in the thin film preparation was calcination with a tube furnace in an ozone atmosphere.

After the fired samples were cooled to room temperature, the thin films were observed under a binocular microscope to determine if cracking or other flaws could be observed. This observation took place after the 320 °C heat treatment as well as after the final calcination. The samples that were observed to have

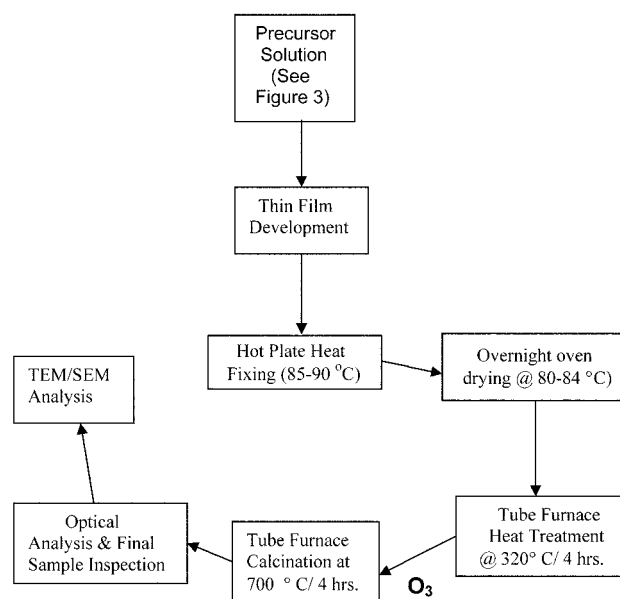


Fig. 4. Flow chart showing the thin film development process.

few or no flaws were submitted for TEM analysis.

Figure 4 shows the flow chart for thin film development after the precursor was synthesized. TEM analysis was used to determine film thickness and size of the crystals. Films fired at various temperatures (600-900 °C) were compared to determine optimum firing temperature to produce an entirely nano-crystalline microstructure.

TEM specimens were prepared using a modified Gatan cross-section method. The samples were broken into small pieces. The small cross section segments were then bonded inside a copper ring 3 mm in diameter and about 1 mm in thickness using Gatan G-1 epoxy. After curing the mixture at 120 °C for 15 minutes, the disc shaped specimen was ground using silicon carbide abrasive papers to about 100 µm in thickness. A Gatan Dimple Grinder and cubic boron nitride pastes were used to form a dimple at the center of the disc. The center of the dimple had a thickness less than 30 µm. A Gatan Precision Ion Polishing System (PIPS) was used to further thin down the dimpled sample until perforation. A 50 nanometre conductive carbon coating was applied using a Gatan Ion Beam Coater (IBC). TEM characterization was conducted using a JEOL 2010 transmission electron microscope, operated at 200 keV. Energy-dispersive X-ray spectra were obtained using an Oxford Instruments EDS system.

Direct analysis of the film using Grazing Incidence X-ray Diffraction (GIXRD) analysis would have been a preferred method. However, since this analytical equipment was not available to us, the bulk polymeric form of the sample was fired at various temperatures and the X-ray data were qualitatively compared for changes in composition. The X-ray results were used to

verify the development of a single-phase final product as well as verify that the composition was consistent with the expected stoichiometry. A bulk sample of the precursor was first fired to 320 °C, and then analyzed with the XRD technique. The sample was then fired to 400 °C and analyzed again and then re-fired and analyzed in 50 °C intervals.

Results and Discussion:

Figure 5 shows typical metal “M” (e.g. Zr, P, Si, Na, etc.) chelation reactions starting with a water-soluble salt and proceeding through polymerization and cross-linking reactions. Good chelation in separate sols (see Fig. 3) helps prevent mixed-cation precipitation during subsequent mixing and heating. Polymerization increases the viscosity and allows for adjustment of the film thickness during spin-coating. Too thick a coating or too much cross-linking can cause cracking of the coating during calcination.

Thermal Analysis Results

Preliminary X-ray analysis of heat-treated tin-precursor bulk powders showed significant crystal development during the lower temperature calcination runs. This observation did not correlate with TEM observations of thin films made from the same composition that were

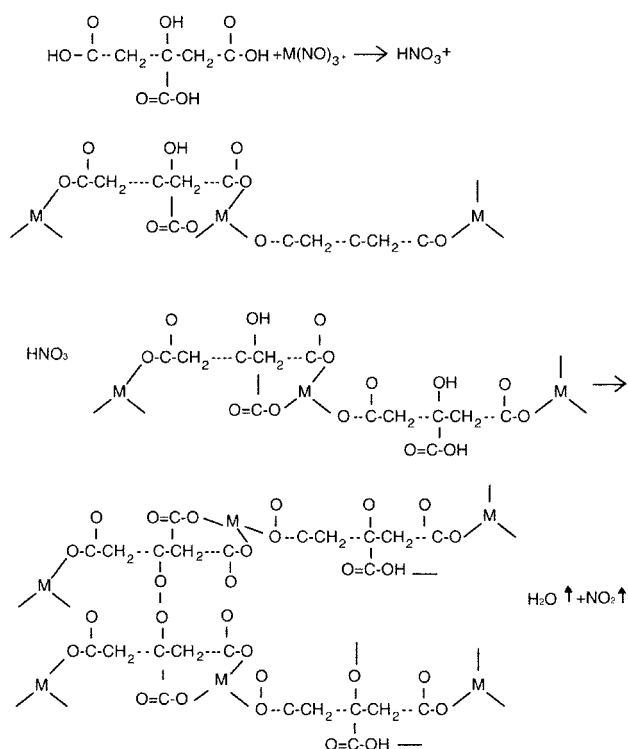


Fig. 5. Chemical Reactions to form organo-metallic “chelates” with metal “M” atoms (Zr, Si, Sn, etc.) in representative polymerization. First reaction is early stage, second reaction removes water as resin is heated.

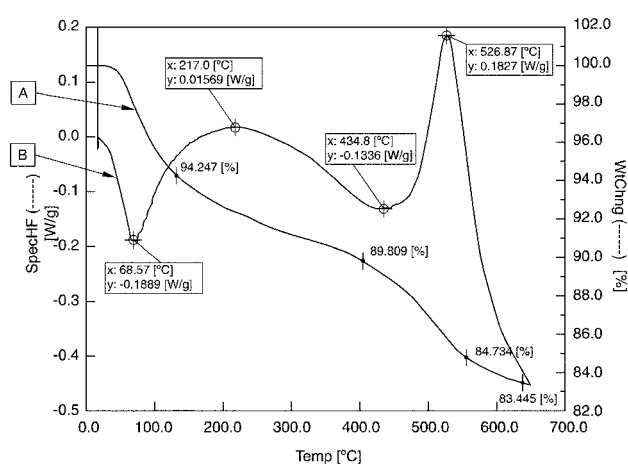


Fig. 6. Thermogravimetric (A) and Differential Thermal Analysis (B) curves.

calcined at the same temperatures. Since the fired-powders were agglomerated into a much greater volume than the thin film precursor, it was speculated that auto-ignition could be taking place. Auto-ignition would cause the powder sample to be internally heated to a significantly higher temperature than the control temperature of the furnace. DTA/TGA analysis was conducted on the powders to help clarify the situation. DTA/TGA analysis was performed on the powder samples that were previously heated up to 320 °C. Air was used instead of ozone because the system could not utilize oxygen or ozone. Figure 6 presents the DTA/TGA curves measured on Sn-precursor material.

Significantly, Figure 6 shows a significant exotherm between 510 and 530 °C. This strengthens the case for an auto-thermal event occurring when calcining a relatively “large” amount of stacked granules of bulk material. The TGA also shows that mass loss is continuous but can be broken down to two events. The first event occurs between 45 and 120 °C. A rapid mass loss occurred between 45 and 120 °C, followed by a slower rate of loss up to 400 °C. This mass loss represented 10.2% of the total. The second event occurs between 400 and 555 °C followed by a slower mass loss between 555 and 660 °C. This region of mass loss on the graph corresponds to a loss of 6.4%. The DTA curve indicated at least four different processes were occurring: two endothermic (at 68 and 434 °C) and two exothermic (at 217 and 527 °C). The first endothermic peak corresponds with a mass loss of 5.75%. This loss can be attributed to tightly bound water and volatile organic carbon. The second endothermic peak at 435 °C corresponds to a bond breaking process of tin, sodium, and phosphorus that were coordinated with carbon, oxygen and hydrogen atoms. This process is to be likely associated with free superficial energy liberation during the bond breaking process of the organic polymer [16]. This hypothesis cannot be confirmed by X-ray analysis because the polymer

material is non-crystalline. The first exothermic event at 217 °C is very broad and is mainly due to the combustion of the precursor carbon. The last exothermic peak at 527 °C is due to the phase transformation of the precursor compounds to the final “Nasicon” metal oxide. New metal to oxygen to metal bonds form in the crystallization process and are associated with an increase in the particle or crystallite size. The DTA curve rapidly drops to the furnace temperature after crystal formation and this demonstrates that oxidation is completed about 650 °C.

In order to demonstrate an auto-thermal exothermic event a relatively large amount of bulk precursor material was stacked to the full level in a small ceramic crucible, and a thermocouple was placed in the sample. The thermocouple was a 0.81 mm diameter, type K that was connected to a laptop computer. The computer program could analyze temperature readings at the rate of four per second in order to accurately record an exotherm. Figure 7 shows the results of heating a 1.055 g sample that completely filled the crucible to a volume of 1.0 millilitre. The temperature was increased at 3 K minute⁻¹ until 600 °C was attained. This temperature was held for two hours and then allowed to cool to room temperature at the rate of 7 K minute⁻¹. An exotherm started to develop nineteen minutes into the heat treatment process at a temperature of 417 °C. The exotherm fully developed its temperature increase thirty minutes into the heat treatment time at a

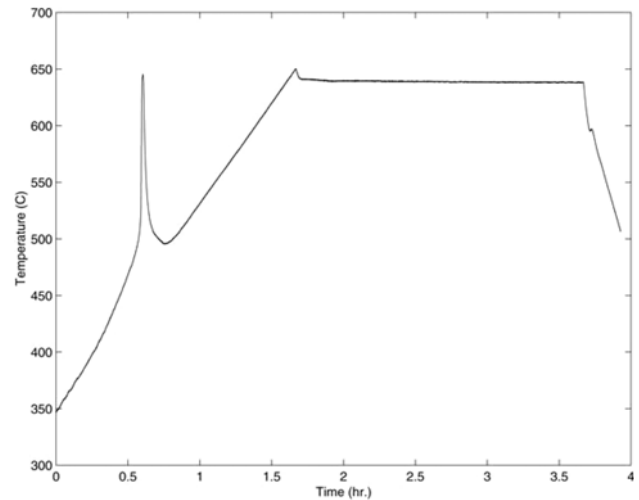


Fig. 7. Temperature plot of tin containing NASICON-type powder as it is calcined from 320 to 650 °C.

temperature of 500 °C. Two minutes and thirty seconds later, the exotherm had reached its temperature limit of 648 °C. After which, the sample temperature dropped back down to 448 °C and maintained the same temperature as the furnace for the duration of the heat treatment process.

For comparison, a small powder sample intended for X-ray analysis was placed in the same type of ceramic crucible described above. This sample had a mass that was two orders of magnitude less than the sample used

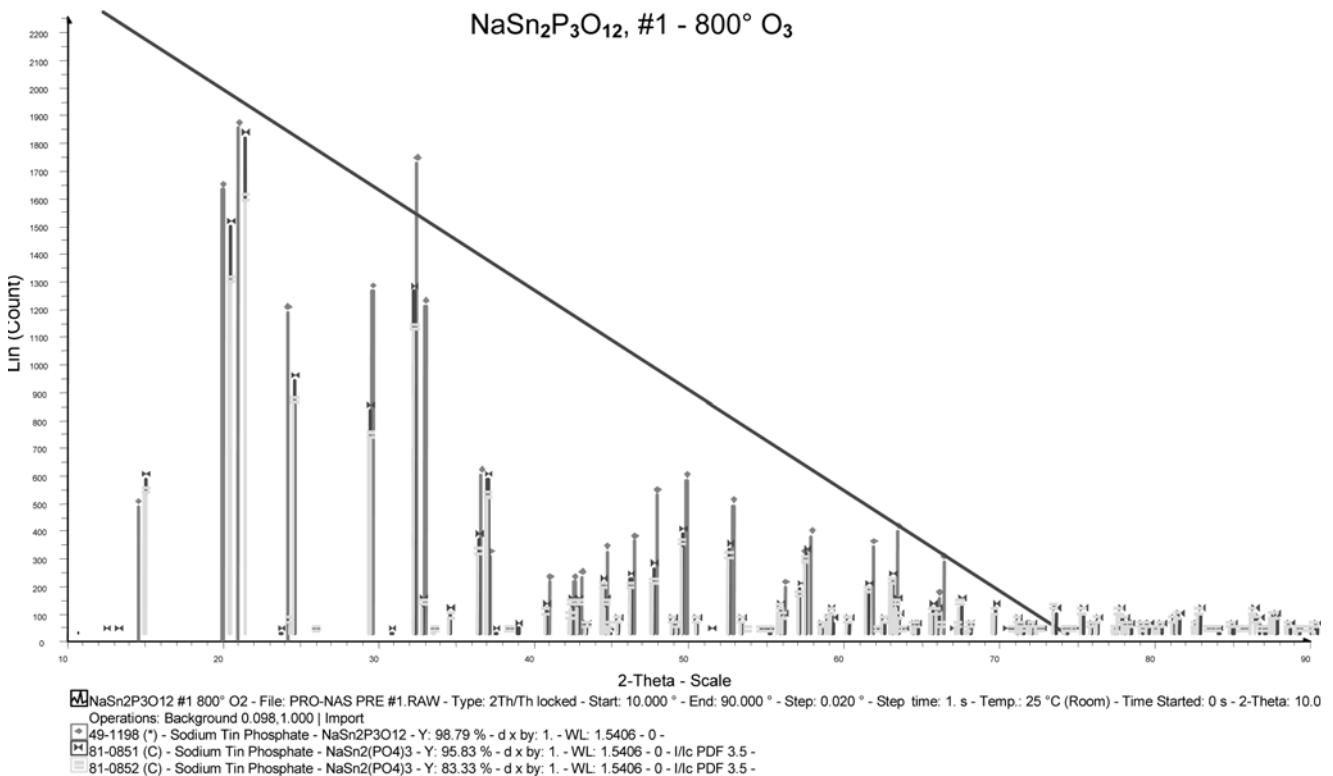


Fig. 8. Tin Containing “NASICON” Powder XRD.

for the DTA analysis. The amount of material heat-treated for XRD barely covered the base of the crucible. A type K thermocouple (same as that described above) was placed into the sample to analyze the sample temperature during the heating process. Using the small amount of powder, no temperature excursions were detected during subsequent heat treatments.

X-ray Powder Diffraction vs. Scanning Electron Microscope Evidence

A portion of the precursor sol (that was not used in the spin coating process) was dried on the hot plate at a maximum temperature of 320 °C, and then heat-treated and calcined (ozone atmosphere), using the same time conditions as the thin films. The XRD pattern of the resulting powder sample is shown in Fig. 8. The X-ray results are typical of those measured on samples that were prepared over a period of several months.

Other bulk powders (after the 320 °C heat treatment) were heated (calcined) to different elevated temperatures and analyzed for changes in the X-ray pattern. There was no shift in the peak locations and no additional peaks appeared as a function of calcining temperature. This indicates transformation of the powder into a single-phase (sodium tin phosphate) ceramic material.

SEM photographs (magnification of 500-1000X) show evidence of defined crystal growth. However, the crystals appear to be interspersed with an amorphous material. Micrographs at higher magnification (12,000-24,000X) showed the crystals averaged between 0.3 to 0.6 micrometres. The average crystal diameter did not change appreciably within the range of calcination temperatures (320-700 °C), and the crystal XRD pattern did not appear to change within this temperature range.

It appeared that an amorphous material surrounded the crystalline material somewhat like a “case and core” configuration. (See figs. 9 and 10). This “case and core” structure was formed every time “chunks” of precursor material were calcined. The material in figures 9 & 10 is from calcined powder samples that were evenly spread as a very thin layer at the base of small alumina crucibles. No auto-thermal temperature excursions were recorded using the small thermocouple in intimate contact with the powder.

Figure 10 shows that there was distinct change in crystal size from the “case” structure to the microcrystalline “core” material. The boundary between crystals and non-crystalline material was very distinct. At present, there is no definitive explanation for this dramatic change in morphology within the same sample of material. Very small amounts of material (less than 0.05 g) were heated in small crucibles to minimize, if not eliminate, the possibility of temperature excursions due to mass heaping of the material. Even when the temperature was measured four times per second with a small thermocouple, no temperature spikes were

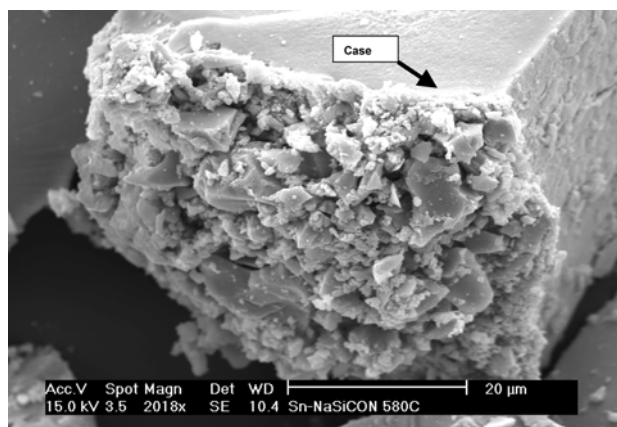


Fig. 9. SEM photo of Sn-Nasicon powder which shows the case-core appearance of the material.

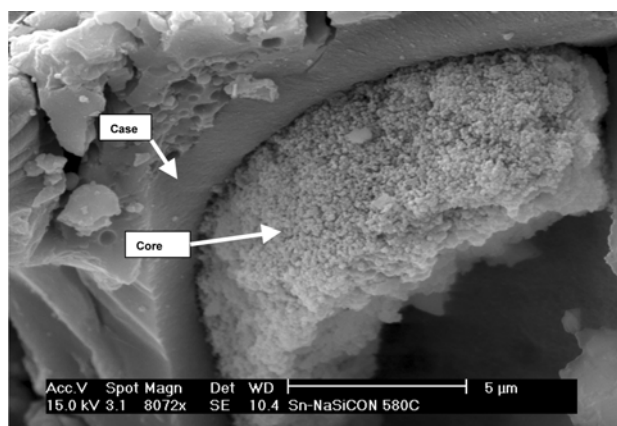


Fig. 10. SEM photo of Sn-NaSiCON powder which shows the noncrystalline “case” and microcrystalline “core” material.

detected. Therefore, it appears that an uncontrolled exothermic reaction (auto-ignition) is not causing the case-core phenomenon.

For the powdered material, an attempt was made to correlate x-ray diffraction line-broadening data with measured particle size data from SEM micrographs. However, no correlation was possible. This was attributed to the presence of multiple-sized crystals, along with non-crystalline material, within the powdered material.

Transmission Electron Microscope (TEM) Results

Silicon substrates that were coated with tin-containing thin films were analyzed by TEM (if the films showed little evidence of cracking as observed under a 20-30X binocular microscope). The results are shown in Fig. 11 where the crystallite size is about 5-10 nanometres. The ring pattern from Selected Area Diffraction is also shown in the figure. This ring pattern is typical for structures that are only nano-crystalline. The ring pattern is observed in thin film samples that were calcined at 700 °C. The pattern was not evident in

samples that were fired at temperatures higher than 700 °C.

The thickness of the film shown in Fig. 11 is about 80 nanometres. This is about one order of magnitude less than the preferred thickness for coating porous electrodes. Lower spinning rates and higher viscosity precursor solutions enhance the ability to produce thicker films. However, there appears to be lower limits to the viscosity and spin rate parameters below which good quality single-layer films cannot be produced. From our experiments, the viscosity limit appears to be at or near 86cP and the lower RPM limit is about 3500. At viscosities below the limit, the precursor solution changes to a thick resin that cannot be spin-cast. When spin-casting at less than 3500 RPM, an uneven film thickness occurs at the edges of the substrate. If significant thickening occurs at the corners of the substrate, cracks develop at the corners during heat treatments.

Thicker coatings can be achieved via multiple coating techniques. Thicker coatings are in the early stages of development in our experiments. However, we have observed that good quality multiple layers depend upon heat treatment techniques and spinning rates that optimize layer thickness and film adhesion.

In summary, calcinations of powders (using equivalent temperature and atmosphere) produce a different result than calcinations of Sn-NaSICON thin films on a silicon substrate. The powders produce crystals that are at least one order of magnitude larger than the crystals produced on a thin film. We speculate that the cause for the smaller crystal sizes in the tin film preparation may be associated with the surface area-to-volume ratio where grains nucleate and grow, but quickly impinge on a surface.

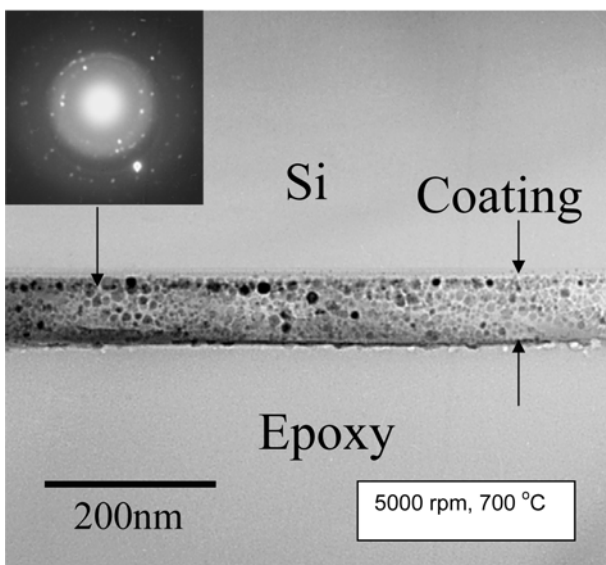


Fig. 11. TEM micrograph of 80 nm (approx.) thick coating on a silicon substrate. A Selected Area Diffraction ring pattern is shown on the upper left.

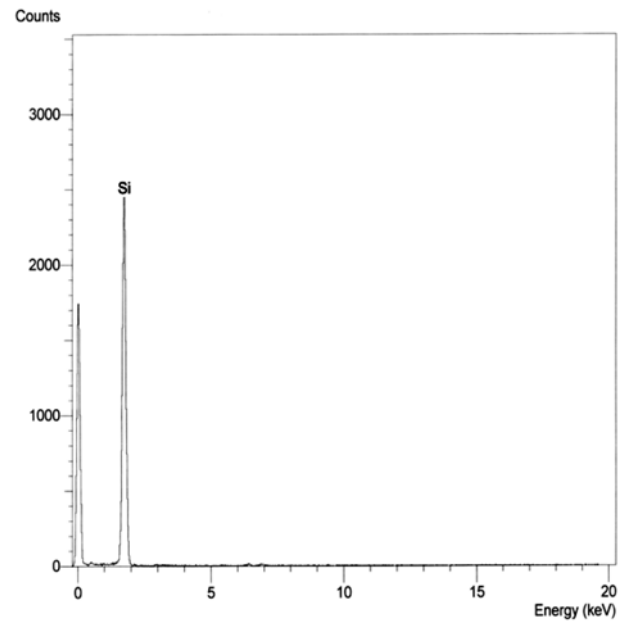


Fig. 12. EDS of Si Substrate below the coating (5000 rpm, 700 °C).

Energy Dispersive X-ray Spectra (EDS) Results

Figure 12 shows the EDS pattern for the silicon substrate. The analysis was taken 50 nm below the thin film. There is no evidence of tin, phosphorus or sodium in the substrate. This implies that those particular elements did not diffuse into the substrate during the

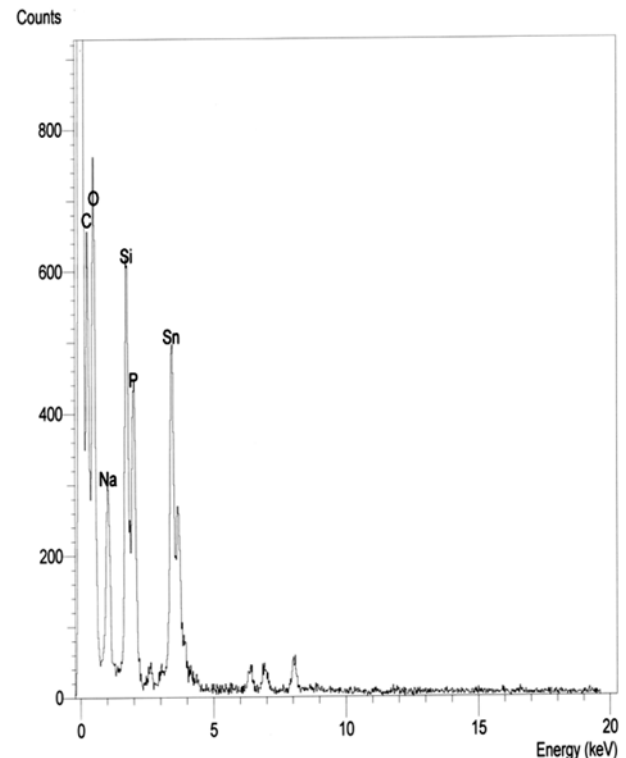


Fig. 13. EDS of coating (5000 rpm, 700 °C).

calcination processes.

The EDS pattern in Fig. 13 shows the elemental components in the thin film that was coated on the same substrate as examined in Fig. 12. The analysis confirms the presence of the elements expected for the thin film (tin, phosphorus, oxygen and sodium). However, all EDS analyses of the thin film revealed silicon. Silicon is expected to easily diffuse into the thin film structure from the substrate since the overall formula, $(\text{Na}_{1+x}\text{Zr}_2\text{Si}_x\text{P}_{3-x}\text{O}_{12})$ ($0 < x < 3$) allows for solid solution substitution of silicon. The ionic radius of silicon is only about 60% of the radius for tin in six-fold coordination with oxygen.

Occasionally, chlorine was found on or near the surface of the thin film. Since chlorine is a byproduct of the tin-containing precursor solution, the presence of trace quantities was not unexpected. It is not known if the small quantity of chlorine will hinder ion transport properties of the thin film.

Conclusions

The Pechini process was successfully used to produce a sodium tin phosphate precursor “resin” without precipitates. This resin was successfully spin cast onto silicon substrates and calcined using ozone to a coherent ceramic thin-film NASICON. Nano-sized crystallites (5-10 nanometres) were produced in the thin films using calcination temperatures of about 600 °C to 700 °C. The thin films showed a consistent thickness, but a single coating thickness was limited to a maximum of about 0.1 micrometres. Preliminary SEM evidence shows that multiple coatings of Sn-NASICON are possible with very little evidence of flaws.

Despite various efforts to control the chemistry, zirconium-containing NASICON thin films were not achieved using the Pechini process due to precipitation problems.

Crystal sizes measured on thin films, using Transmission Electron Microscopy, did not correlate to crystal sizes (measured using Scanning Electron Microscopy) from bulk powder “chunks” that were produced under the same atmosphere and temperature calcinations conditions. There was evidence of auto-thermal heating resulting in a temperature excursion during calcination of large stacks of resin precursor chunks. However, “case-core” grain size morphology was also observed in small pieces of ground resin that was thinly spread during calcinations where small thermocouples could not detect temperature excursions. Thin films coatings

appeared to provide physical constraints conducive to the formation of nano-crystals at temperatures at about 600 °C to 700 °C, while the “bulk” powder forms various larger crystal sizes arranged in an unusual “case-core” morphology.

Acknowledgement

The authors wish to thank Jan-Fong Jue for his technical support regarding TEM and EDS analysis on this project and Arnold W. Erickson for performing the X-ray Diffraction experiments. This work was supported by the U.S. Department of Energy, under DOE Idaho Operations Office Contract CE-AC07-99ID13727.

References

1. I. Kosacki, P.L. Colomban, V. Petrovsky, and H.U. Anderson, Paper A3-010-00, Annual Meeting of the American Ceramic Society, St. Louis, May, 2000.
2. B.P. Gorman and H.U. Anderson, Paper A3-040-00, Annual Meeting of the American Ceramic Society, St. Louis, May, 2000.
3. M. Nogami, H. Matsushita, T. Kasuga, and T. Hayakawa, *Electrochemical and Solid-State Letters* 2[8] (1999) 415-417.
4. C.K. Kuo, A. Tan, P. Sarkar, and P.S. Nicholson, *Solid State Ionics* 58 (1992) 311-314.
5. G. Schafer, A.V. Zyl, and W. Weppner, U.S. Patent 5,474,959, Dec. 12, 1995.
6. G.W. Schafer, H.J. Kim, and F. Aldinger, *Solid State Ionics* 97 (1997) 285-289.
7. A.V. Joshi, M. Liu, A. Bjorseth, and L. Renberg, U.S. Patent 5,290,405 March 1, 1994.
8. O. Damasceno, E. Siebert, H. Khireddine, and P. Fabry, *Sensors and Actuators B* 8 (1992) 245-248.
9. R.C.T. Slade and K.E. Young, *Solid State Ionics* 46 (1991) 83-88.
10. “PRONAS” available from Ceramatec, Inc., 2425 South 900 West, Salt Lake City, UT 84119; Phone 801-978-2152.
11. S. YDE-Anderson, J.S. Lundsgaard, L. Moller, and J. Engell, *Solid State Ionics* 14 (1984) 73-79.
12. A. Caneiro, P. Fabry, H. Khireddine, and E. Siebert, *Analytical Chemistry* 63[22] (Nov. 15, 1991) 2550-2557.
13. Y. Shimizu and T. Ushijima, *Solid State Ionics* 132[1-2] (Jul 2000) 143-148.
14. P.A. Lessing, *Bulletin American Ceramic Society* 68[5] (1989) 1002-1007.
15. E.R. Losilla, M.A.G. Aranda, S. Bruque, J. Sanz, M.A. Paris, J. Campo, and A.R. West, *Chem. Mater.* [12] (2000) 2134-2142.
16. M. Picquart, L. Escobar-Alarcon, E. Torres, T. Lopez, and E. Haro-Poniatowski, *Journal of Materials Science* 37 (2002) 3241-3249.